MOVING TARGET TRACKING OF UAV/UGV HETEROGENEOUS SYSTEM BASED ON QUICK RESPONSE CODE

Xiao LIANG[1], Guodong CHEN[2], Shirou ZHAO[3], Yiwei XIU[4]

By the characteristics of UAV (Unmanned Aerial Vehicle) and UGV (Unmanned Ground Vehicle), UAV/UGV heterogeneous systems can accomplish many complex tasks cooperatively. Moving target tracking is an important basis for the relative positioning and formation maintenance of the system. This paper first designs a UAV/UGV collaborative heterogeneous system. Then, a control method of quadrotor is proposed which is based on SBUS protocol to simulate remote control (RC) in order to maintain the original stability of UAVs. A UGV with Mecanum wheel and its control method is presented. For the problems of real-time performance and occlusion, a tracking scheme based on QR Code (Quick Response Code) identification is proposed. Finally, the scheme is applied to the heterogeneous systems. Simulation and experimental results show that the proposed method is suitable for UAV/UGV heterogeneous system to perform the collaborative tracking task.

Keywords: UAV/UGV collaborative system; moving target tracking; Analog RC; Meconium UGV; QR Code

1. Introduction

With the rapid development of science and technology, the applications of aerial robots (also known as unmanned aerial vehicles, UAV) and ground robots (unmanned ground vehicle, UGV) are getting more and more attention form researchers all over the world. Recently, UAV/UGV heterogeneous system[1-3] has become a hot topic. In UAV/UGV heterogeneous system, insufficient real-time performance and accuracy will lead to failures in collaboration. Therefore, the target tracking algorithm is an important basis for UAV/UGV to make relative positioning and formation [4,5]. Since the attitude, scale, occlusion, and light are

[1] Prof., School of Automation, Shenyang Aerospace University, China, e-mail: connyzone@126.com
[2] Eng., School of Automation, Shenyang Aerospace University, China, e-mail: 1536716822@qq.com
[3] Eng., School of Automation, Shenyang Aerospace University, China, e-mail: 490531633@qq.com
[4] Eng., School of Automation, Shenyang Aerospace University, China, e-mail: 296663653@qq.com

constantly changing during the movement, many researches have been carried out about target tracking.

Moving target recognition and tracking mainly include the following classic methods: Frame difference method [6], Meanshift algorithm [7], optical flow method [8]. The method of frame difference calculation is fast, and usually used in camera calibration. Meanshift is simple and easy to implement, but it's hard to track the target with high speed. The optical flow method carries a wealth of motion information and three-dimensional information, and the calculation amount is huge, which usually cannot meet real-time demand. Most of above algorithms cannot find the target again after losing it. Therefore, the method combining detection and tracking are studied, such as TLD (Tracking-Learning-Detection) [9]. TLD algorithm achieves long-term tracking of single targets and solves the problem of losing target which is caused by target deformation and partial occlusion. However, in global search, the real-time performance is not satisfactory. The correlation filtering algorithm adopts the local search method which has obvious advantages in real-time performance, but it is difficult to track the target with high speed and longer occlusion time, such as KCF (Kernel Correlation Filter) [10] based on HOG feature.

This paper firstly introduces a UAV/UGV heterogeneous system. Then a quadrotor control method based on SBUS protocol to simulate remote control is proposed. The design and control of UGV with Mecanum wheel are also introduced. In order to improve the real-time performance and accuracy, a tracking scheme based on QR Code [11] is proposed. In experiment, the tracking scheme is loaded into the performed UAV/UGV heterogeneous systems and the result shows that the proposed method is suitable for collaborative tracking task.

2. UAV/UGV heterogeneous system

UAV loaded with the camera and other sensors which can obtain a two-dimensional horizontal image of the environment in front of UGV. It supplements the obstacle information in front of UGV, so it can provide local/global image information for UGV obstacle avoidance. On the basis of mutual awareness of UAV/UGV, heterogeneous system can achieve complex tasks such as cluster formation, avoidance guidance and information fusion. (Fig. 1).

In Fig. 1, the gray block in the diagram is relative positioning and it is particularly critical for heterogeneous system. Although GPS (Global Positioning System) can achieve relative positioning of two types of unmanned devices, the accuracy is low. Collaborative positioning becomes an important bridge which connects UAV and UGV for the heterogeneous collaboration system to complete collaborative tasks. Collaborative positioning requires video and image processing, so the tracking accuracy and real-time performance are the key issues that must be solved.

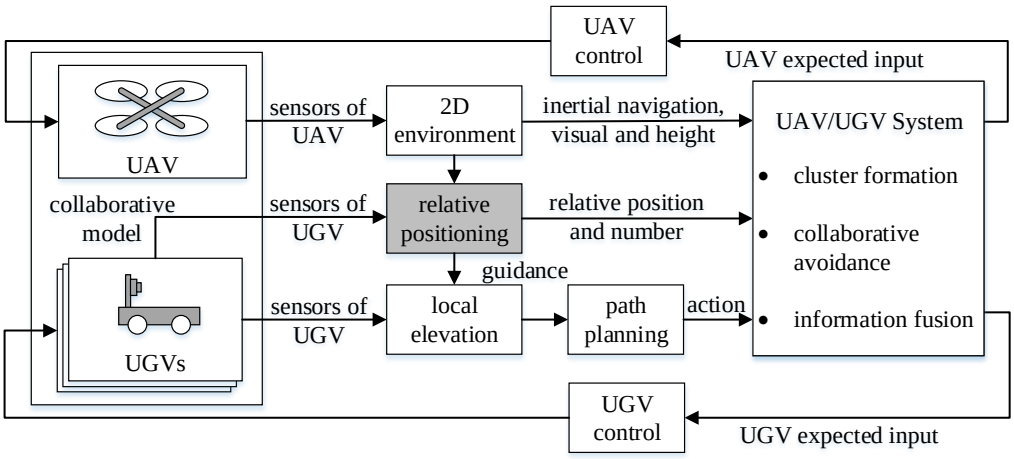

Fig. 1. UAV/UGV heterogeneous system

3. Design and control of UAV

The UAV used in the heterogeneous system is a quadrotor. The main structure consists of a frame, four motors, four electronic governors, a signal translator, a flight controller and a wireless communication equipment. Accelerometer, gyroscope, magnetometer, barometer on the flight controller can realize attitude solving. So as to the signal translator. The hardware structure is shown in Fig. 2.

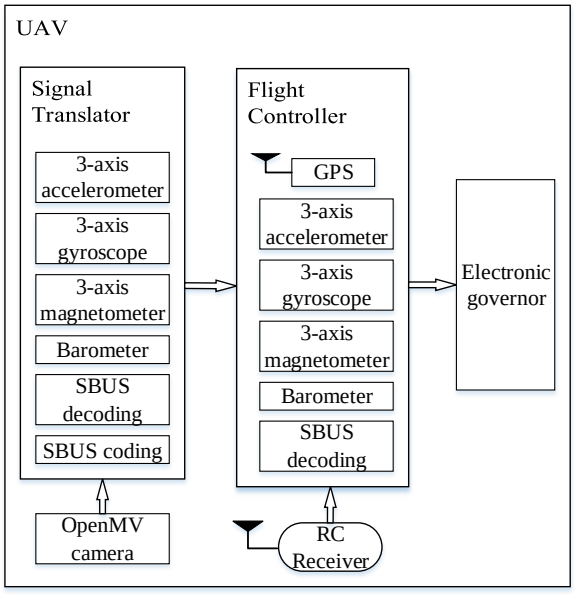

Fig. 2. UAV hardware structure

OpenMV camera can acquire the images in real time and send the processed coordinates to the UAV. The UAV automatically tracks the target according to the coordinates. In this system, RC (Remote control) has the highest control right and can be switched to manual mode at any time. When the UAV loses its target, it ensures the safe of the system.

3.1 UAV modeling and automatic control

In this paper, assuming that the quadrotor is rigid and symmetrical, and the origin of the body frame is consistent with the center of gravity, the quadrotor dynamics model can be described as [12]:

$$\begin{cases} \ddot{x} = u_1(\cos\psi \sin\theta \cos\phi + \sin\psi \sin\phi) + d_x \\ \ddot{y} = u_1(\sin\psi \sin\theta \cos\phi - \cos\psi \sin\phi) + d_y \\ \ddot{z} = u_1 \cos\theta \cos\phi - g + d_z \\ \ddot{\phi} = u_2 \\ \ddot{\theta} = u_3 \\ \ddot{\psi} = u_4 \end{cases} \tag{1}$$

Where θ is pitch angle, ψ is yaw angle, ϕ is roll angle, g is gravitational acceleration, and d_x, d_y and d_z are the additional disturbances caused by the external force. The total thrust on the z-axis is expressed as $u_1 = \sum_{i=1}^{4} F_i / m$, where m is the mass of the quadrotor and $F_i\,(i = 1, 2, 3, 4)$ is the thrust of the four rotors. u_2 and u_3 are the pitch and roll inputs respectively, and u_4 represents the yawing moment.

There are many researches on quadrotor control. The paper adopts a classic PID control algorithm [13], because PID control has the advantages of simple structure, easy operation, good robustness and achievability.

3.2 Analog RC based on SBUS protocol

In order to maintain the original stability of UAV and reduce the workload of developing flight control, the paper introduces an analog remote control based on the SBUS protocol. The method uses a signal generation device to simulate the remote-control signals to control UAV. A Pixhawk2 flight controller is used in UAV and connected to a signal translator (Fig. 3). The functions in signal translator are used to decode and encode the input signal of RC and generate the control signal for flight controller, so as to realize automatic/semi-automatic control of the UAV.

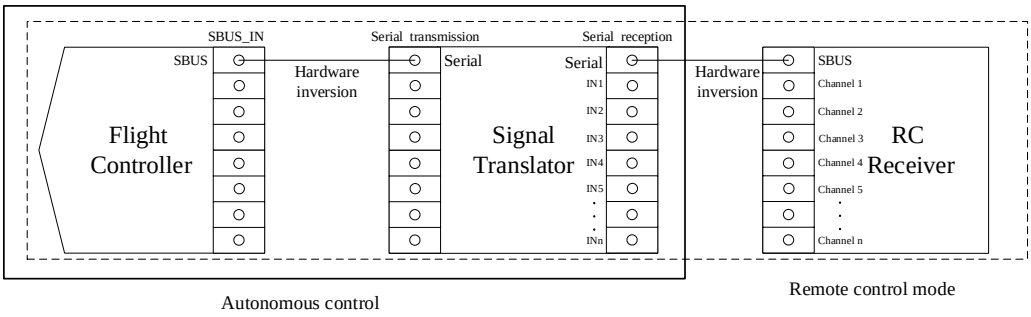

Fig. 3. structure diagram of quadrotor control system

The UAV has three flight modes: manual RC mode, automatic flight mode and emergency stop mode. The flow chart of control is shown in Fig. 4.

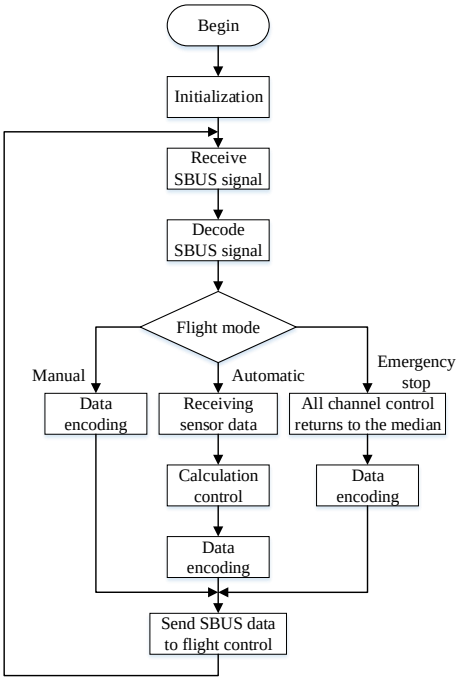

Fig. 4. UAV flight mode control flow chart

(1) manual RC mode

The receiver receives remote control data in real time and sends it to the Signal Translator through the SBUS protocol. The Signal Translator decodes and encodes the data and sends the received data to flight controller through SBUS protocol as usual, to achieve the purpose of manual control flight.

(2) automatic flight mode

The Signal Translator decodes the data transmitted from the receiver but does not perform the code transmission to flight controller. Instead, the controller calculates the signal of each channel, and then encodes and transmits these signals to achieve the purpose of automatic flight.

(3) emergency stop mode

The Signal Translator immediately sets all channel values to the middle value, then encodes and sends them to achieve the purpose of UAV fixed-point hovering to ensure flight safety.

4. Design and control of UGV

The UGV is mainly composed of a car body, 4 motors and their drives, a main control board and wireless communication equipment. (Fig. 5).

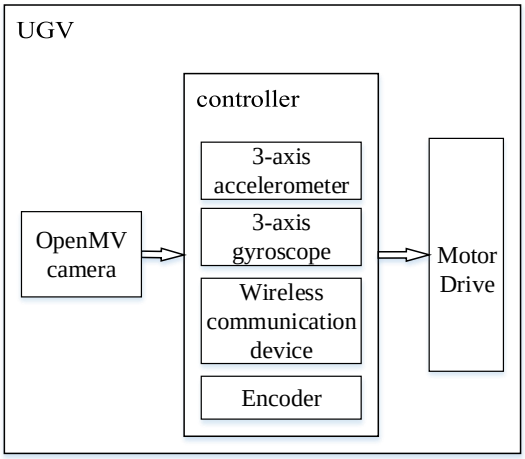

Fig. 5. UAV flight mode control flow chart

OpenMV camera can acquire images in real time and transmit the processed coordinates to UGV. Then, UGV tracks and moves to the target autonomously.

4.1 Modeling and control of UGV

To simplify the mathematical model of kinematics, there are some assumptions:

(1) The omnidirectional wheel will not slip, and the ground has sufficient friction;

(2) Four wheels are distributed on four corners of the rectangle or square, and wheels are parallel to each other.

Assuming that the body coordinate system coincides with the geographic coordinate system, the Mecanum UGV motion direction is specified in Fig. 6.

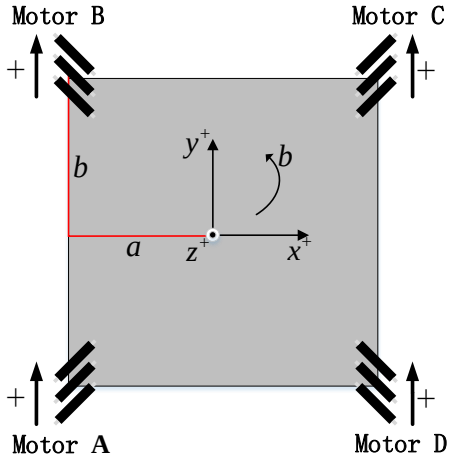

Fig. 6. Mecanum UGV motion pattern

According to Fig. 8, the motion of UGV can be linearly decomposed into three components. V_A、V_B、V_C and V_D represents the velocity of four wheels Motor A、Motor B、Motor C and Motor D, respectively. V_x is the velocity of UGV along X-axis, V_y is the velocity of UGV along the Y-axis and ω is the angular velocity around Z-axis. Here, a is half the width of the UGV and b is half the length of the UGV.

When UGV goes along X-axis, there is:

$$\begin{cases} V_A = -V_x \\ V_B = +V_x \\ V_C = -V_x \\ V_D = +V_x \end{cases} \tag{2}$$

When UGV goes along Y-axis, there is:

$$\begin{cases} V_A = +V_y \\ V_B = +V_y \\ V_C = +V_y \\ V_D = +V_y \end{cases} \tag{3}$$

When the car rotates around its geometric center, there is:

$$\begin{cases} V_A = -\omega(a+b) \\ V_B = -\omega(a+b) \\ V_C = +\omega(a+b) \\ V_D = +\omega(a+b) \end{cases} \tag{4}$$

Basing on Equation (2), (3) and (4), the velocity of four wheels can be calculated according to the status of UGV.

$$\begin{cases} V_A = -V_x + V_y - \omega(a+b) \\ V_B = +V_x + V_y - \omega(a+b) \\ V_C = -V_x + V_y + \omega(a+b) \\ V_D = +V_x + V_y + \omega(a+b) \end{cases} \tag{5}$$

By C language, the input parameters are V_x, V_y and ω, then the speeds of four motors are calculated and sent to the PID controller of UGV.

4.2 Control mode of UGV

UGV has two control schemes, and they are remote and automatic control. Each control scheme has two motion modes and they are speed and displacement mode. Remote control mode receives data by remote control or mobile phone. Automatic mode receives the commands transmitted by other controllers through the serial port.

4.2.1 Speed control mode

When UGV is in speed control mode, the format of speed control data in each frame is shown in Table 1. According to Fig. 6, Tx[1] controls the speed of the A motor; Tx[2] controls the speed of the B motor; Tx[3] controls the speed of the C motor; and Tx[4] controls the speed of the D motor.

Table 1

Format of speed control data

Data field	Tx[0]	Tx[1]	Tx[2]	Tx[3]
Contents	Mode	Motor A speed control	Motor B speed control	Motor C speed control
Data field	Tx[4]	Tx[5]	Tx[6]	Tx[7]
Contents	Motor D speed control	Default	Default	Direction control bit

4.2.2 Displacement control mode

When UGV is in displacement control mode, displacement is input. Mecanum UGV automatically performs kinematic analysis and converts displacement to speed. A 16-bit unsigned number synthesized by Tx[1] and Tx[2] controls the X-axis displacement; A 16-bit unsigned number synthesized by Tx[3] and Tx[4] controls the Y-axis displacement; A 16-bit unsigned number

synthesized by Tx[5] and Tx[6] controls the Z-axis displacement. The format of coordinate-displacement control data in each frame is shown in Table 2.

Table 2

Format of displacement control data

Data field	Tx[0]	Tx[1]	Tx[2]	Tx[3]
Contents	Mode	High 8 bits of X-axis displacement control	Low 8 bits of X-axis displacement control	High 8 bits of Y-axis displacement control
Data field	Tx[4]	Tx[5]	Tx[6]	Tx[7]
Contents	Low 8 bits of Y-axis displacement control	High 8 bits of Z-axis displacement control	Low 8 bits of Z-axis displacement control	Direction control bit

5. Tracking scheme based on Apriltag

It is well known that QR Code is a plane figure consist of black and white small blocks which can store information. The more blocks, the more information. In order to reduce the amount of calculation, this paper uses Apriltag [14] as the tracking scheme. Apriltag uses a simple QR Code which has only 4 to 12 bits data and can be detected more robustly and from longer ranges. Apriltag [15] is an improved visual positioning system based on ARToolkit[16] and ARTag [17]. It is a visual reference library [18] and widely used in robots and UAV positioning guide [19].

Apriltag not only can identify and track the target, but also can get the 3D pose of the target. As long as the camera resolution, focal length and the size of tag are known, the algorithm can identify the type, ID, distance and attitude of tag.

5.1 Detection and identification of Tags

The Tag is a quadrangle which is inner black and outer white, as shown in Fig. 7.

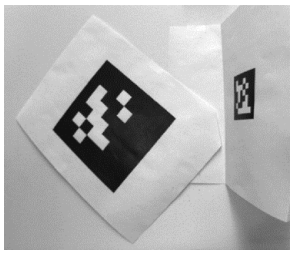

Fig. 7. Tags

The tag detection algorithm begins by computing the gradient at every pixel, including their magnitudes (Fig. 8(a)) and direction (Fig. 8(b)). Using a graph-based method, pixels with similar gradient directions and magnitude are

clustered into components (Fig. 8(c)). By using weighted least squares, a line segment is then fit to the pixels in each component (Fig. 8(d)). The direction of the line segment is determined by the gradient direction, so that segments are dark on the left, light on the right.

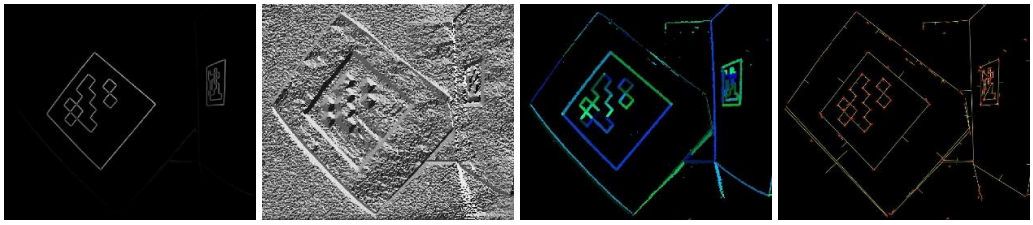

(a) (b) (c) (d)

Fig. 8. Detection process

At this point, the Tag is transformed into a set of directed segments, and then the sequence of segments of the quadrilateral is calculated. The method used is based on a recursive depth-first search with a depth of 4[14].

5.2 Calculation of the distance and angle from Tag to camera

In homography transformation (one plane is mapped to another) and external parameter estimation, a 3×3 homography matrix (A conversion matrix when mapping, and the matrix is usually represented by H) needs to be calculated. It maps the coordinate system of the Tag to a 2D image coordinate system. Homography matrix is calculated by Direct Linear Transform (DLT) algorithm. The position and orientation of the Tag require additional information, namely the focal length of camera and the physical size of Tag. The 3×3 homography matrix can be written as the product of a camera projection matrix P with 3×4 order and an external parameter matrix E with 4×3 order. The external parameter matrix is usually 4×4 steps, and each position satisfies $z=0$ in coordinate system of Tag. Therefore, the coordinates of Tag can be rewritten as a two-dimensional homogeneous point by deleting the third column of matrix P to form a truncated external parameter matrix. The rotational component of E is represented as R_{ij} and the translational component is represented as T_k. s is scale factor, so:

$$H=\begin{bmatrix} h_{00} & h_{01} & h_{02} \\ h_{10} & h_{11} & h_{12} \\ h_{20} & h_{21} & h_{22} \end{bmatrix} = sPE = s\begin{bmatrix} f_x & 0 & 0 & 0 \\ 0 & f_y & 0 & 0 \\ 0 & 0 & 1 & 0 \end{bmatrix}\begin{bmatrix} R_{00} & R_{01} & T_x \\ R_{10} & R_{11} & T_y \\ R_{20} & R_{21} & T_z \\ 0 & 0 & 1 \end{bmatrix} \tag{6}$$

Here h_{ij} is the element of homography matrix H. f_x and f_y are the focal length of camera respectively. It is not possible to solve E directly because P is

not full rank. By calculating the right side of Eq. 6, each h_{ij} can be written into a set of equations:

$$\begin{cases} h_{00} = sR_{00} f_x \\ h_{01} = sR_{01} f_x \\ h_{02} = sT_x f_x \\ \cdots \end{cases} \tag{7}$$

The elements of R_{ij} and T_k can be easily determined. Each column of the rotation matrix must be a unit vector, so the limitation can be satisfied by different s. Since the rotation matrix has only two columns, s can be set as the geometric mean of the amplitude of matrix. Because the columns of rotation matrix must be orthogonal, the third column can be recovered by computing the cross product of two known columns.

The above DLT process and normalization process cannot guarantee that the rotation matrix is strictly orthogonal. So, to solve this problem, R can be decomposed by polar coordinates to generate a Frobenius matrix norm with minimum error.

Finally, by homography matrix, the relative coordinate system of tag is mapped to the coordinate system of image. Furthermore, the distance and angle from Tag to camera are finally obtained.

6. Simulation and experiment

6.1 Simulation of tracking target

KCF is a common tracking algorithm and it is used to make comparison with Apriltag. KCF abstracts the tracking problem into a linear regression model. In order to adapt to the deformation of target, KCF is modeled by ridge regression which has the feature of regularization. The objective function of the ridge regression is:

$$\min_w \sum_i (f(x_i) - y_i)^2 + \lambda \|w\|^2 \tag{12}$$

Here, λ is a regularization parameter. Calculate the derivative of Eq. 12 about w and let it equal to zero. So the extreme value is:

$$w = (X^T X + \lambda I)^{-1} X^T y \tag{13}$$

In Eq. 13, each row of X represents x_i, y is a Gaussian regression label and I is an identity matrix. Eq. 13 can be written as a complex domain form:

$$w = (X^H X + \lambda I)^{-1} X^H y \tag{14}$$

X^H is a complex conjugate transpose matrix. In order to avoid calculating the inversion of matrix and accelerate the calculation, Eq. 14 is transformed to Fourier domain.

$$\hat{w} = \frac{\hat{x}\Theta\hat{y}}{\hat{x}^*\Theta\hat{x} + \lambda} \tag{15}$$

In Eq. 15, $\hat{x}$ is a fast Fourier transform of x, and $\hat{y}$ is a fast Fourier transform of y, Θ represents the hadamard product.

After running KCF, select the tag36h11_1 tag as the initial frame (Fig. 9(a)), and Apriltag also selects the tag36h11_1 tag as the tracking target (Fig. 9(b)).

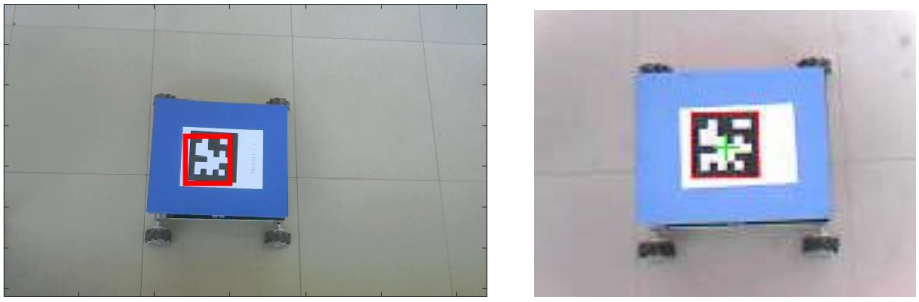

(a) Initial frame of KCF (b) Initial frame of Apriltag

Fig. 9. Initial frame of KCF and Apriltag

After the selection of initial frame, both algorithms can accurately identify and track the target. In order to improve the running speed of Apriltag in embedded devices, the resolution is appropriately reduced. So there is more noise in Fig. 9(b), but it does not affect the accuracy of recognition.

If occlusion occurs, the results of KCF and Apriltag are shown in Fig. 10. When occlusion just occurs, KCF can still determine the probable location of target in Fig. 10(a), but Apriltag will lose target in Fig. 10(b). It is because that KCF uses real-time online training to handle occlusion problems. Once target is occluded, Apriltag will lose some features, so tracking failed.

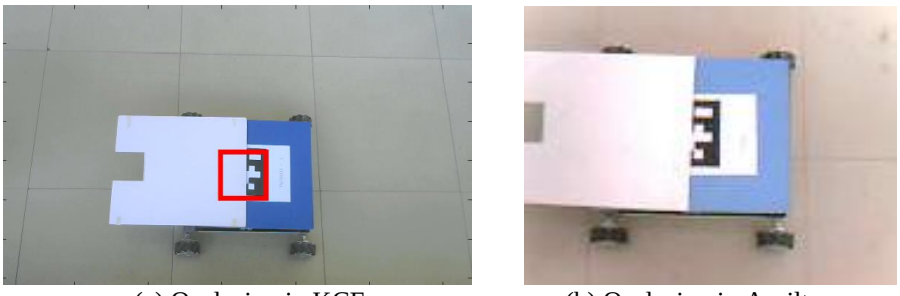

(a) Occlusion in KCF (b) Occlusion in Apriltag

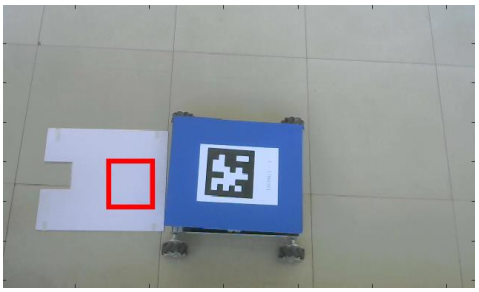
(c) KCF loses target after occlusion

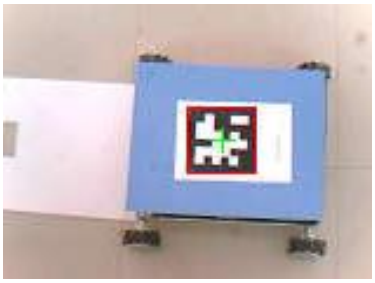
(d) Apriltag still tracks target after occlusion

Fig. 10. Occlusion in KCF and Apriltag

After occlusion for a short period of time, KCF loses target in Fig. 10(c). Instead, Apriltag still tracks target (Fig. 10(d)). The comparison in Fig. 10 shows that Apriltag can re-identify and track the target as soon as occlusion is removed.

6.2 Tracking experiment

6.2.1 Tracking experiment of UGV

UGV uses flat view to track target and target moves in a complex background. If target is lost, UGV will stop moving. PTZ (Pan, Tilt, Zoom) camera will rotate to making global search until camera detects the target again.


(a) Tracking the target with linear motion

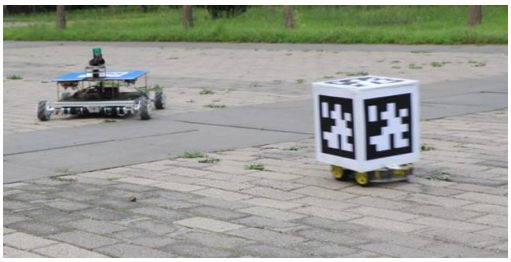
(b) Target starts turning


(c) Target moves in a circular orbit

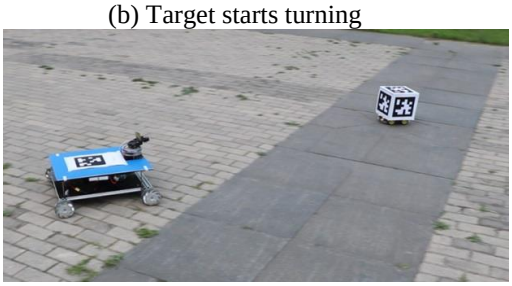
(d) Target moves out of the circular orbit

Fig. 11. Tracking experiment of UGV

Fig. 11 shows that UGV can adjust the speed according to the distance from target, so the distance between UGV and target is basically unchanged. Fig. 11(b), (c), (d) is a set of turning test. Because UGV is equipped with four

omnidirectional wheels and the rotation angle of pan/tilt is 180°, tracking experiment of UGV is satisfactory.

6.2.2 Collaborative tracking experiment of UAV/UGV

UAV uses top view of UGV. When target is lost, UAV will enter hover mode and wait for the target to reappear or the RC command.

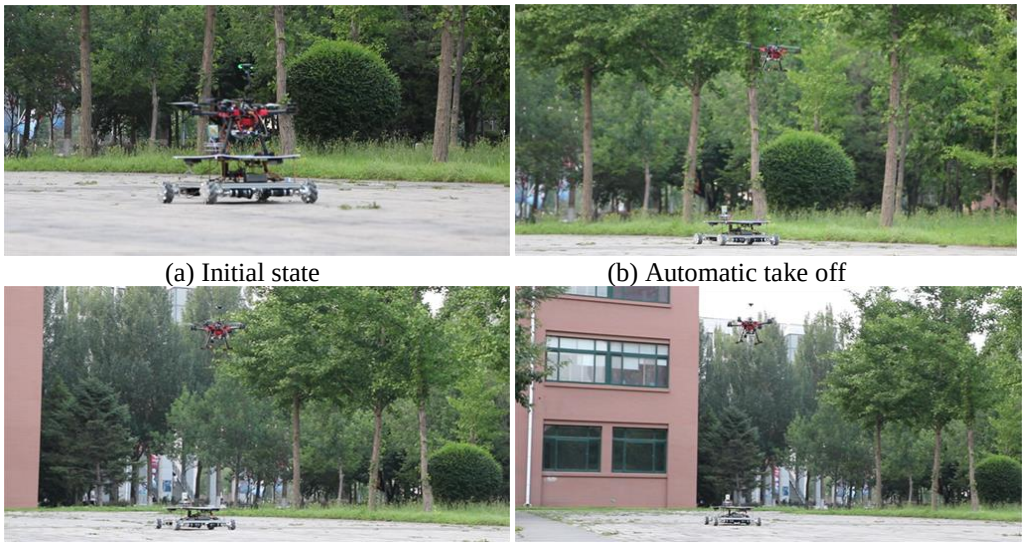

(a) Initial state (b) Automatic take off

(c) Selection of initial frame (d) Tracking target

Fig. 12. Tracking experiment of UAV

In initial state, UAV parks on UGV as shown in Fig. 12(a). In Fig. 12(b), UAV takes off automatically and flies to a predetermined altitude. Fig. 12(c) and (d) show that the proposed method can help UAV/UGV heterogeneous system to complete the moving target tracking task successfully.

7. Conclusions

This paper uses a UAV/UGV heterogeneous system to complete a moving target tracking task. Firstly, the UAV/UGV heterogeneous system is introduced. Then, an analog remote control based on the SBUS protocol is proposed for UAV. Next, a UGV with omnidirectional wheel is also designed for the heterogeneous system. To improve the effectiveness and accuracy of tracking, a tracking scheme based on QR Code is studied. The following conclusions are obtained through simulation and experiment.

1. Analog remote control based on the SBUS protocol can maintain the original stability of UAV and reduce the workload of developing.

2. UGV has a variety of control modes to adapt to different tasks. Omnidirectional wheels enable UGV to meet multiple challenges from various environments.
3. The tracking scheme based on QR Code runs well in embedded devices. The effectiveness and accuracy are satisfied. The scheme is suitable for UAV/UGV heterogeneous system to track moving target.

Acknowledgment

This work is supported by National Natural Science Foundation of China under Grant 61503255, Aeronautical Science Foundation of China under Grant 2016ZC54011 and Natural Science Foundation of Liaoning Province under Grant 2015020063. The authors also gratefully acknowledge the helpful comments and suggestions of the reviewers, which have improved the presentation.

The authors declare that there is no conflict of interest regarding the publication of this article.

R E F E R E N C E S

[1]. Haibin D, Senqi L. Research on heterogeneous collaborative technology of air/ground robots: status quo and prospects [J]. Chinese science, 2010, 40(9):1029-1036.

[2]. Hager C E, Kwon H, Zarzhitsky D, et al. A cooperative autonomous system for heterogeneous unmanned aerial and ground vehicles[A]. Infotech at Aerospace, 29-31 March 2011, AIAA 2011-1487.

[3]. Grocholsky B, Keller J, Kumar V, et al. Cooperative air and ground surveillance: A scalable approach to the detection and localization of targets by a network of UAVs and UGVs[J]. IEEE Robot Autom Mag, 21 August, 13(3):16-25, 2006.

[4]. Wenzel K E, Masselli A, Zell A. Automatic Take off, Tracking and Landing of a Miniature UAV on a Moving Carrier Vehicle[J]. Journal of Intelligent and Robotic Systems, March, 61(1-4):221-238, 2011.

[5]. Cheng H, Cheng Y S, Li X K, et al. Autonomous Takeoff, Tracking and Landing of a UAV on a Moving UGV Using onboard Monocular Vision[C]. Proceedings of the 32nd Chinese Control Conference, Xi'an, China, 21 October, 1934-1768, 2013.

[6]. Ramya P, Rajeswari R. A Modified Frame Difference Method Using Correlation Coefficient for Background Subtraction[J]. Procedia Computer Science, December, 93:478-485, 2016.

[7]. Youness Aliyari Ghassabeh, Frank Rudzicz. The mean shift algorithm and its relation to kernel regression[J]. Information Sciences, 20 June, 348:198-208, 2016.

[8]. Tianding C, Jian H, Chao L, et al. Moving target tracking using sparse optical flow method[J]. Advanced Materials Research, 2013, 718-720:2335-2339.

[9]. Linbao X, Shuming T, Jinfeng Y, et al. Robust autonomous car-like robot tracking based on tracking-learning-detection[J]. Applied Mechanics and Materials, 2014, 687-691:564-571.

[10]. Le Z, Ponnuthurai Nagaratnam S. Robust visual tracking via co-trained kernelized correlation filters[J]. Pattern Recognition, 2017, 69:82-93.

[11]. Nazemzadeh P, Fontanelli D, Macii D, et al. Indoor localization of mobile robots through QR code detection and dead reckoning data fusion[J]. IEEE/ASME Transactions on Mechatronics, December 22(6):2588-2599, 2017.

[12]. Dailiang M, Yuanqing X, Ganghui S, et al. Flatness-based Adaptive Sliding Mode Tracking Control for a Quadrotor with Disturbances[J]. Journal of the Franklin Institute, July, 355(14), 2018.
[13]. LIU Jin-kun. Advanced PID Control and MATLAB Simulation[M]. Beijing: Electronic Industry Press, 2004.
[14]. Olson E. AprilTag: A robust and flexible visual fiducial system[C]. 2011 IEEE International Conference on Robotics and Automation, Shanghai, China, May 9-13, 2011.
[15]. Sagitov A, Shabalina K, Sabirova L, et al. ARTag, AprilTag and CALTag fiducial marker systems: comparison in a presence of partial marker occlusion and rotation[C]. 14th International Conference on Informatics in Control, Automation and Robotics, Madrid, Spain, July 26-28, 2017
[16]. Dawar Khan, Sehat Ullah, Ihsan Rabbi. Factors affecting the design and tracking of ARToolKit markers[J]. Computer Standards & Interfaces, 2015, 41(C):56-66.
[17]. Celozzi C, Paravati G, Sanna A, et al. A 6-DOF ARTag-based tracking system[J]. IEEE Transactions on Consumer Electronics, 2010, 56(1):203-210.
[18]. Bergamasco F, Albarelli A, Torsello A. Pi-Tag: a fast image-space marker design based on projective invariants[J]. Machine Vision and Applications, 2013, 24(6):1295-1310.
[19]. Hartley R, Kamgar-Parsi B, Narber C. Using roads for autonomous air vehicle guidance[J]. IEEE Transactions on Intelligent Transportation Systems, 2018, 19(12):3840-3849.